NANO LETTERS

2008
Vol. 8, No. 5
1318-1322

# UV-Light Induced Fabrication of $CdCl_2$ Nanotubes through CdSe/Te Nanocrystals Based on Dimension and Configuration Control

**Jie Zeng,[†] Chi Liu,[‡] Jianliu Huang,[‡] Xiaoping Wang,*[,†,§] Shuyuan Zhang,[†] Gongpu Li,[†] and Jianguo Hou*[,†]**

*Hefei National Laboratory for Physical Sciences at the Microscale, University of Science and Technology of China, Hefei 230026, Anhui Province, China, Department of Chemistry, University of Science and Technology of China, Hefei 230026, Anhui Province, China, Department of Physics, University of Science and Technology of China, Hefei 230026, Anhui Province, China*

*Received December 20, 2007; Revised Manuscript Received February 21, 2008*

## ABSTRACT

**Since the discovery of $WS_2$ nanotubes in 1992 (*Nature* 1992, *360*, 444), there have been significant research efforts to synthesize nanotubes and fullerene-like hollow nanoparticles (HNPs) of inorganic materials (*Nat. Nanotechnol.* 2006, *1*, 103) due to their potential applications as solid lubrications (*J. Mater. Chem.* 2005, *15*, 1782), chemical sensing (*Adv. Funct. Mater.* 2006, *16*, 371), drug delivering (*J. Am. Chem. Soc.* 2005, *127*, 7316), catalysis (*Adv. Mater.* 2006, *18*, 2561), or quantum harvesting (*Acc. Chem. Res.* 2006, *39*, 239). Nanotubes can be produced either by rolling up directly from layer compounds (*Nature* 2001, *410*, 168) or through other mechanisms (*Adv. Mater.* 2004, *16*, 1497) such as template growth (*Nature* 2003, *422*, 599) and decomposition (*J. Am. Chem. Soc.* 2001, *123*, 4841). The Kirkendall effect, a classical phenomenon in metallurgy (*Trans. AIME* 1947, *171*, 130), was recently exploited to fabricate hollow 0-D nanocrystals (*Science* 2004, *304*, 711) as well as 1-D nanotubes (*Nat. Mater.* 2006, *5*, 627). Although the dimension of resulting hollow nanostructures depends on precursors, the hollow nanomaterials can also be organized into various dimensional nanostructures spontaneously or induced by an external field. In this letter, we report, for the first time, the UV-light induced fabrication of the ends-closed 1-D $CdCl_2$ nanotubes from 0-D CdSe solid nanocrystals through the Kirkendall effect and the head-to-end assembled process. Our results demonstrate the possibility to control the dimension (0-D to 1-D) and the configuration (solid to hollow) of nanostructures simultaneously and have implications in fabricating hollow nano-objects from zero-dimensional to multidimensional.**

The morphology and assembly of nanostrucures in the chemical synthesis processes can be feasibly controlled and modified by the external parameters such as magnetic field,[15] optical, and electric.[16] Recently, we have reported the one-pot fabrication of Au (Pt or Pd) hollow nanoparticle chains from cobalt nanoparticles through the magnetic field guiding assembly and in situ galvanic replacement reactions.[17] On the basis of the above cases,[1−14] here we select UV light as another external field to induce the fabrication of 1-D $CdCl_2$ nanotubes from 0-D nanocrystals. Two features are combined in our new method to fabricate the inorganic nanotubes. One is the Kirkendall effect, which is particularly effective for formation of hollow nanostructures.[13] The other is the interaction between the electric dipoles, which can effectively induce the assembly for nanostructures.[18,19]

In the experiment, we start with CdSe nanocrystals and *o*-dichlorobenzene to prepare the $CdCl_2$ nanostructure. Wurtzite CdSe nanocrystals were synthesized by the procedure developed by Peng[20] with some modifications.[21] *o*-Dichlorobenzene was used as solvent, which could produce the chlorine free radicals from the photolysis process.[22] CdSe nanocrystals with the size of 2.2 nm was dissolved in *o*-dichlorobenzene and dropped onto the substrate of amorphous carbon under the irradiation of germicidal UV lighting. After 2 h reaction, the sample was air-dried in the dark and transferred to transmission electron microscopy (TEM) for structural analysis.

It is found that most of the as-prepared nanostructures exhibit tubular structures with uniform wall thicknesses. Parts a−c of Figure 1 show some representative images of these nanotubes. As seen, the nanotubes have inner diameters

* Corresponding authors. E-mail: xpwang@ustc.edu.cn (X.P.W.); jghou@ustc.edu.cn (J.G.H).

[†] Hefei National Laboratory for Physical Sciences at the Microscale.

[‡] Department of Chemistry, University of Science and Technology of China.

[§] Department of Physics, University of Science and Technology of China.

10.1021/nl0733334 CCC: $40.75 
**Published on Web 04/05/2008**

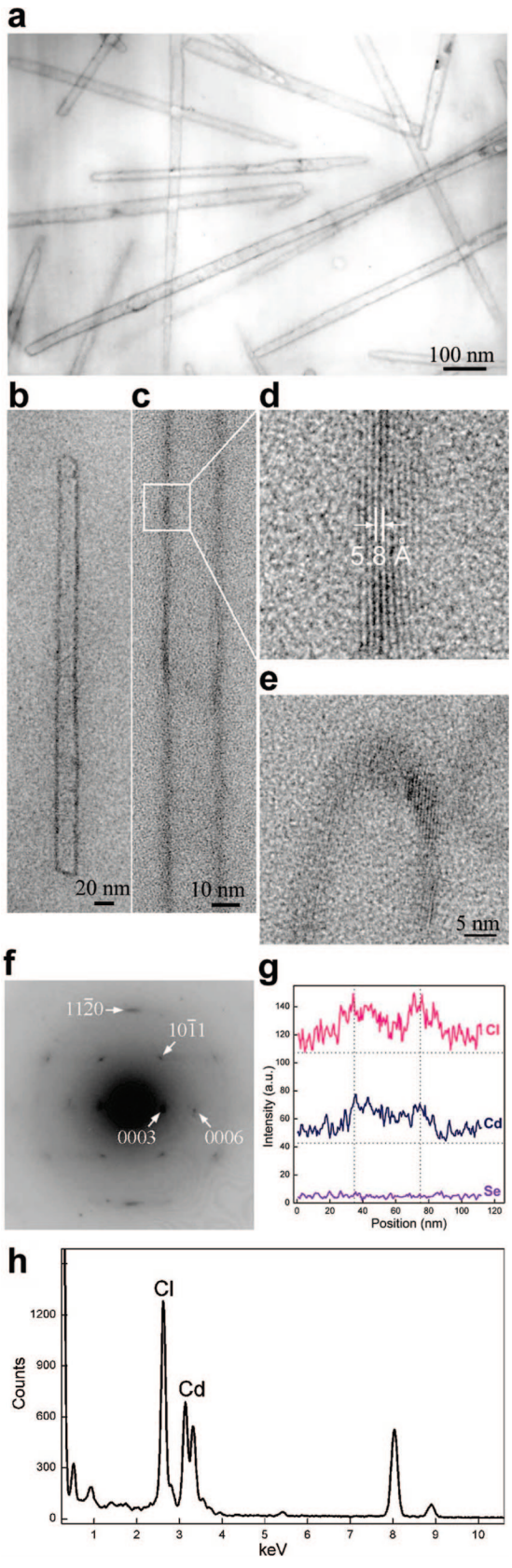


**Figure 1.** Structural characterization of $CdCl_2$ nanotubes. (a−c) TEM images of the $CdCl_2$ nanotubes. (d) HR-TEM images of the marked part of (c) and (e), the end of a tube. (f) SAED pattern of the nanotube in (c) along the [11$\bar{2}$0] zone axis. (g−h) Compositional line profile across a nanotube with about 40 nm width and the EDX spectroscopy.

ranging from 7 to 60 nm and wall thicknesses between 2 and 5 nm. Almost all of the tubes have two ends closed. Energy dispersive X-ray (EDX) spectroscopy shows that the nanotubes are made up of cadmium and chlorine elements, and no selenium element can be found within the uncertainty of the experiment (Figure 1h). Compositional line profile shows well-correlated Cd and Cl signals across the tube walls (Figure 1g), indicating the formation of stoichiometric $CdCl_2$ during the reaction. The structural characteristic of the nanotube can also be observed clearly in the high-resolution TEM (HR-TEM) images (Figure 1d−e) and select-area electron diffraction (SAED) pattern (Figure 1f), which results indicate the nanotube being well crystalline.

The SAED pattern shows the typical diffraction features of a cylindrical nanotube and can be interpreted as an addition diffraction pattern originated from the different areas of the nanotube. The two strong {0003} spots correspond to the diffraction from the planes of the side walls. The six {11$\bar{2}$0} spots are produced by the second prismatic planes perpendicular to the upper and lower walls of the nanotube, whereas two of the stronger spots that are at 90° with respect to {0003} spots can also be produced by the side walls. Four {10$\bar{1}$1} spots are gained from inclined planes. It can be deduced that the nanotube is oriented along the [11$\bar{2}$0] zone axis of the rhomb-center $CdCl_2$ structure (Supporting Information Figure 1). The (0003) plane in the stem of the nanotube is parallel to the tube axis, and its lattice spacing of 0.58 nm can be readily resolved on the high-resolution TEM images (Figure 1d). Note that the lattice planes of the close end of the nanotube are also (0003) planes and parallel to the tube axis, which are apparently different from the frizzy lattices of most type of inorganic nanotubes.[1,23] The above results indicate that we have successfully prepared $CdCl_2$ nanotubes from nanocrystals in room temperature and atmosphere environment. It should be pointed out that the method to fabricate the $CdCl_2$ nanotubes from nanocrystals under soft chemical conditions reported here is in sharp contrast to all previous studies on inorganic nanotubes. Most of the previous studies on the formation of inorganic nanotubes have been based on methods with high temperature, high pressure, or inert ambience.[24] Also, the results usually were made up of different forms besides nanotubes.

To elucidate the mechanism of the process, we have investigated the morphology and the structure of the sample within different formation stages of the nanotubes. Figure 2a shows the TEM image of the starting CdSe nanocrystals with the average size of 2.2 nm. After 5 min of irradiation under a UV lamp, the nanocrystals convert into HNPs with the size from 7−60 nm (Figure 2b). EDX analysis indicates the hollow nanoparticles being composed by Cd and Cl with the mol ratio of about 1:2.03, and HR-TEM implies that the hollow $CdCl_2$ nanoparticles are amorphous (Supporting Information Figure 2). It should be emphasized that the process of nanocrystals converted into HNPs can not occur without the irradiation of UV light.

Figure 2c shows the products after 20 min UV irradiation. It can be observed clearly that some hollow nanorods as well as several sphere-like hollow particles have formed. Interest-

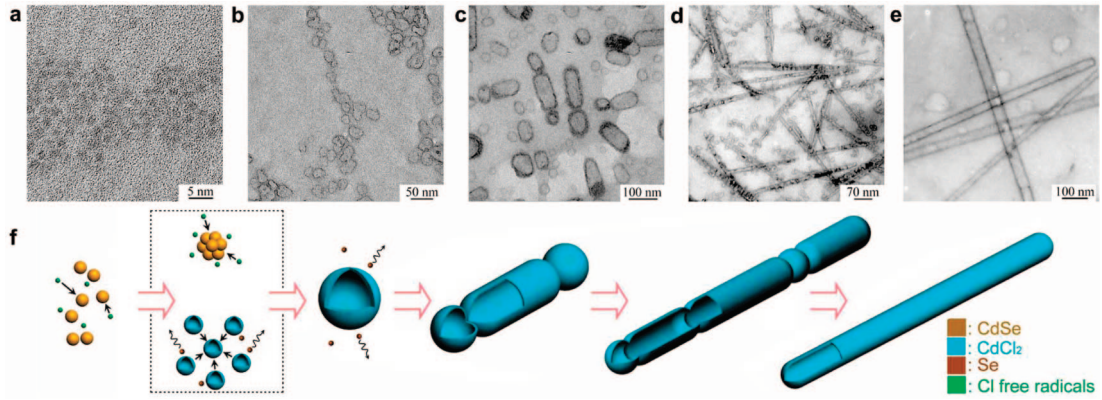


**Figure 2.** Evolution of $CdCl_2$ nanotubes with time by UV irradiation of CdSe nanocrystals with the size of 2.2 nm in *o*-dichlorobenzene. (a−e) TEM images of obtained samples at 0, 5, and 20 min, and 1 and 2 h, respectively. (f) Schematic illustration of the formation process of $CdCl_2$ nanotubes from 2.2 nm CdSe nanocrystals.

ingly, many hollow nanoparticles assemble one by one or attach to the end of hollow nanorods. HR-TEM images show that most of the hollow nanorods and particles are crystalline (Supporting Information Figure 3). After 1 h irradiation, the embryo of nanotubes are formed (Figure 2d), and after two hour's reaction, nearly perfect nanotubes are obtained (Figure 1 and Figure 2e).

On the basis of the results shown in Figure 2, we consider that the formation process of nanocrystals–to-nanotubes is probably completed via two stages: one is the transformation from nanocrystals into HNPs and the other is the assembly of HNPs into nanotubes.

We attribute the cause of the first stage (nanocrystals convert into HNPs) to the Kirkendall effect, which can create the hollow structures in the solid through the interdiffusion between different elements driven by their asymmetry concentration.[13] The detailed chemical reactions can be described as following:

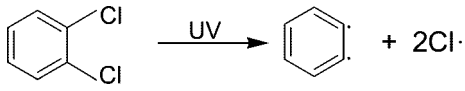


$$CdSe + 2Cl\cdot \xrightarrow{UV} CdCl_2 + Se$$

In this stage, the active Cl free radicals (Cl•) are first produced from photolysis of *o*-dichlorobenzene under the irradiation of UV lamp.[22] Then solid CdSe nanocrystals containing Cl free radicals in an appropriate dilute solution brings an additional concentration asymmetry of Cd and Se elements between the core of nanocrystals and the solution. The large concentration difference provides a great driving force of the outward diffusion for the core species, and consequently the $Cd^{2+}$ and $Se^{2-}$ ions will diffuse outward. Because of their different ion radius, 0.95 Å for $Cd^{2+}$ and 1.98 Å for $Se^{2-}$,[25] $Cd^{2+}$ will diffuse outward from the core much faster than $Se^{2-}$ and react with the Cl free radicals to produce $CdCl_2$, as shown in Figure 2f. The process results in the formation of $CdCl_2$ shells and the collapse of Se species in nanocrystals core. Furthermore, the residual Se species can diffuse through the shells readily because $CdCl_2$ hollow nanoparticles are most likely amorphous in the initial stage (Supporting Information Figure 2). Noted that the initial nanoparticles diameter is about 2.2 nm, whereas the hollow particles have an averaged diameter around 40 nm, therefore many particles have to be combined to form the much bigger hollow particles. This may happen in two ways (Figure 2f). First, solid particles agglomerate to form a fairly big solid particle, which then is transformed into a big hollow particle. Alternatively, the small solid particles are transformed into small hollow particles, which then agglomerate. It is also observed that the shape of hollow $CdCl_2$ nanoparticles in Figure 2b are not sphere-like, which may imply the congregating products of several nanoparticles. This irregular hollow $CdCl_2$ nanostructure can further drive itself into a sphere-like one by release of its surface energy.

Taking into account the behavior that the nanotubes can not be formed without the irradiation of UV light, we temporally ascribe the mechanism of the stage of HNPs into nanotubes to the light-induced dipole–dipole interaction between the HNPs. Under that driven by the interaction, the HNPs can assemble via head-to-end along the [11$\bar{2}$0] direction and form the nanotubes as shown in Figure 2c−d. During this stage, it is considered that the process of mass transfer between the conjoined HNPs and the crystal reconstruction of primary nanotube will occur to further decrease the interfacial energy and improve the structure of the nanotubes.

Because the structures of HNPs are mostly amorphous, it appears that the crystallization occurs in the course of the tube formation. This can probably completed through the attachment and incorporation processes of HNPs to the crystal orientation of the already existing tube. It is reasonable to presume that the atomic mobility of amorphous HNPs is fairly higher than that of a crystalline one. We consider that it is this high atomic mobility to ensure the attachment and incorporation processes of HNPs to form the nanotube segment. The other related question in the above process is how all of the tubular segments have exactly the same crystalline orientation while attaching to each other. As seen in the Figure 2c, one can find that even when most of the nanotube segments are prone to attach head to end while

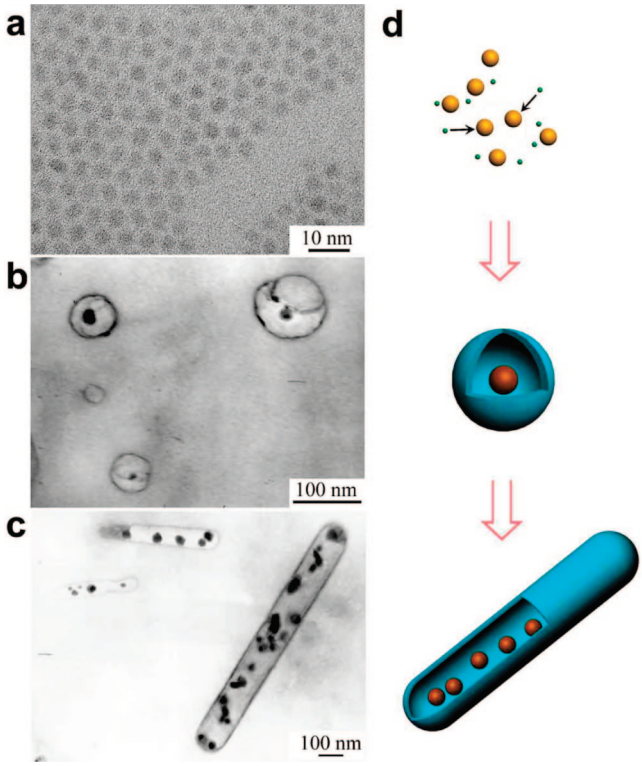


**Figure 3.** Controlled diffusion processes starting from CdSe nanocrystals with the size of 4.0 nm. (a) TEM image of the starting CdSe nanocrystals (4.0 nm). (b−c) TEM images of the obtained nanostructures at 0.5 (named nanoprisons) and 3 h under UV irradiation. (d) Schematic diagram of the case of 4.0 nm CdSe nanocrystals as precursor.

being parallel to the long axis, there still exists a twist in the orientation between the various segments. The phenomenon can also be observed in Supporting Information Figure 3A,B. To incorporate various segments along the same direction, it is necessary to rotate the twisted segment and even displace the tubular segment, as shown in the schematic illustration of Supporting Information Figure 3C. The force to drive the above motions of nanotube segments is probably supplied by the strong dipole–dipole interaction between the segments. Supporting Information Figure 4 shows the schematic of attachment and incorporation processes for tubular segments and TEM images of two kinds of transitional states, which also demonstrates the high mobility of the atoms indirectly. Additionally, we suspect that the UV irradiation may enhance the unusual high mobility of the atoms of HNPs and the dipole–dipole interaction between the segments because the nanotube can not form without the UV light irradiation. However, more works are needed in the future to answer these questions.

To investigate the diffusion process for a double element compound more carefully, we carry out another fabrication process from CdSe nanocrystals with bigger size of about 4.0 nm (Figure 3a). After 30−40 min irradiation, a type of yolk−shell nanostructure forms (Figure 3b). We name it "nano-prisons", which contain an *intelligent* criminal each. We are not able to identify the exact component of the criminal, for it is quite unrestful in the TEM measurement. The activity of two nanoprisons was tracked through TEM

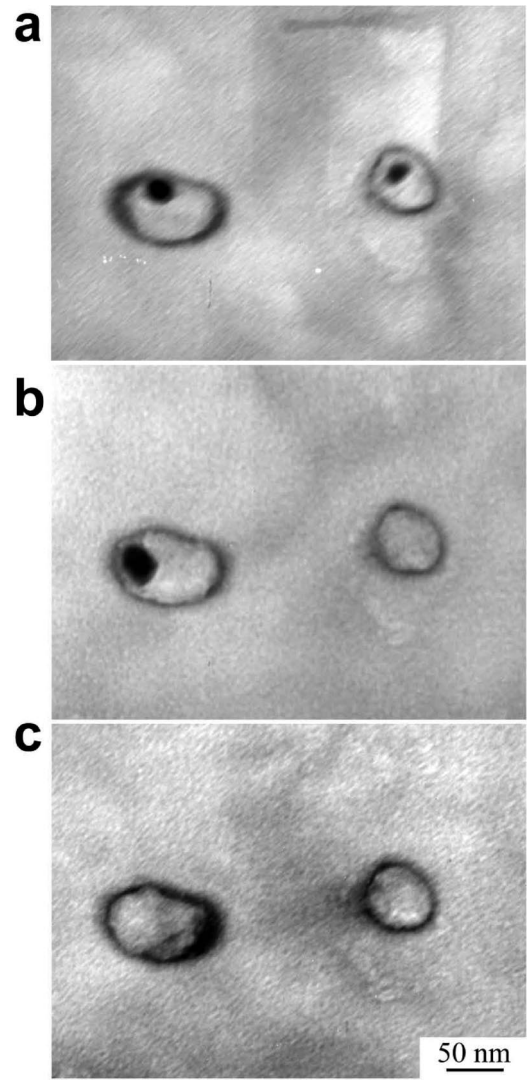


**Figure 4.** TEM tracking process of two nanoprisons under electric beam irradiation. (a−c) TEM tracking images with the focused time of 0, 2, and 5 min, respectively.

photography (Figure 4a−c). It is very interesting that a "prison break" process occurrs under the irradiation of TEM electronic beam. Within 2 min, one criminal disappeared and the other was still encaged. After 5 min, the second criminal also escaped successfully. We presume that the criminal is amorphous selenium (*a*-Se), because both the fast diffusion of $Cd^{2+}$ and the collapse of Se species will result in disorder of survivals. Furthermore, the low melting point (50 °C for *a*-Se and 217 °C for gray-Se) and the high vapor pressure (1 Pa at 227 °C) of selenium solid ensure quick and complete removal of the nanoprisons, for it will be very effeminate under an electronic beam. The very similar phenomenon was also observed in another system.[26] The demonstration of yolk−shell nanostructures also supports the presumption of the Kirkendall effect. Analogously, nanotubes with the criminals inside can be obtained after 3 h reaction under the UV light irradiation (Figure 3c, for schematics, see Figure 3d). We notice that both the size of nanoprisons and the width of final tubes are larger than those in the instance with 2.2 nm CdSe nanocrystals as the starting material (Figure 1).

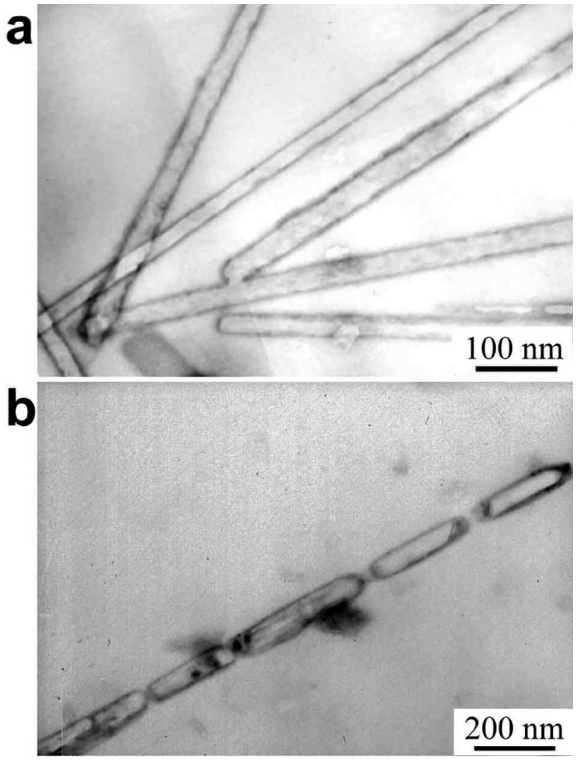


**Figure 5.** Extending cases of $CdCl_2$ nanotubes. (a) TEM image of $CdCl_2$ nanotubes starting from 2.0 nm CdTe nanocrystals. (b) TEM image of head-to-end self-assembly structure of five tubes.

The result also suggests that more hollow particles are prone to inosculation to reduce the additional energy.

Above result indicates that the nanotube-like morphology of the production can be readily controlled by the selection of the original particle sizes as well as the reaction time. This synthetic procedure can also be extended through other types of nanocrystals: blende CdTe nanocrystals with a size of ~2.0 nm were used as starting materials to produce $CdCl_2$ nanotubes successfully in an analogous process (Figure 5a) that is even more uniform.

In conclusion, the ends-closed 1-D $CdCl_2$ nanotubes can be fabricated from 0-D CdSe/Te solid nanocrystals through a UV-light induced approach that involves the Kirkendall effect and the head-to-end assembled process. The observations indicate that the dimension and configuration of nanostructures can be controlled simultaneously. It is demonstrated that the orientable assembled technique can serve as the motivity of constructing 1-D nanostructures through dimensional expansion, not only for nanowires[18] but also for nanotubes. Furthermore, the light-induced method not only has potential application for fabrication of inorganic fullerene-like nanostructures in mild conditions, it is also an effective approach for head-to-end self-assembly. Figure 5b shows the TEM image of a five nanotube arrangement forming a chain along the same axis, whereas the usual alignment for one-dimensional nanostructures aggregation is side to side.[27]

**Acknowledgment.** We are grateful to W. Lu and T. McIntyre for discussions. This work was supported by the National Key Basic Research Program (Grant No. 2006CB922002) and Natural Science Foundation of China (Grant Nos. 50721091, 50532040, 90406009, 60676030).

**Supporting Information Available:** Methods; preparation of starting materials; synthesis of $CdCl_2$ nanotubes and HNPs. This material is available free of charge via the Internet at http://pubs.acs.org.

## References

(1) Tenne, R.; Margulis, L.; Genut, M.; Hodes, G. *Nature* **1992**, *360*, 444–446.
(2) Tenne, R. *Nat. Nanotechnol.* **2006**, *1*, 103–111.
(3) Rapoport, L.; Fleischer, N.; Tenne, R. *J. Mater. Chem.* **2005**, *15*, 1782–1788.
(4) Liu, A. H.; Wei, M. D.; Honma, I.; Zhou, H. S. *Adv. Funct. Mater.* **2006**, *16*, 371–376.
(5) Son, S. J.; Reichel, J.; He, B.; Schuchman, M.; Lee, S. B. *J. Am. Chem. Soc.* **2005**, *127*, 7316–7317.
(6) Cheng, F. Y.; Chen, J.; Gou, X. L. *Adv. Mater.* **2006**, *18*, 2561+.
(7) Goldberger, J.; Fan, R.; Yang, P. D. *Acc. Chem. Res.* **2006**, *39*, 239–248.
(8) Schmidt, O. G.; Eberl, K. *Nature* **2001**, *410*, 168–168.
(9) Remskar, M. *Adv. Mater.* **2004**, *16*, 1497–1504.
(10) Goldberger, J.; He, R.; Zhang, Y.; Lee, S.; Yan, H.; Choi, H.-J.; Yang, P. *Nature* **2003**, *422*, 599–602.
(11) Nath, M.; Rao, C. N. R. *J. Am. Chem. Soc.* **2001**, *123*, 4841–4842.
(12) Smigelskas, A. D.; Kirkendall, E. O. *Trans. AIME* **1947**, *171*, 130–142.
(13) Yin, Y.; Rioux, R. M.; Erdonmez, C. K.; Hughes, S.; Somorjai, G. A.; Alivisatos, P. *Science* **2004**, *304*, 711–714.
(14) Fan, H. J.; Knez, M.; Scholz, R.; Nielsch, K.; Pippel, E.; Hesse, D.; Zacharias, M.; Gösele, U. *Nat. Mater.* **2006**, *5*, 627–631.
(15) Singamaneni, S.; Bliznyuk, V. *Appl. Phys. Lett.* **2005**, *87*, 162511.
(16) Ma, L. C.; Subramanian, R.; Huang, H.-W.; Ray, V.; Kim, C.-U.; Koh, S. J. *Nano Lett.* **2007**, *7*, 439–445.
(17) Zeng, J.; Huang, J.; Lu, W.; Wang, X.; Wang, B.; Zhang, S.; Hou, J. *Adv. Mater.* **2007**, *19*, 2172–2176.
(18) Tang, Z. Y.; Kotov, N. A.; Giersig, M. *Science* **2002**, *297*, 237–240.
(19) Tang, Z. Y.; Zhang, Z. L.; Wang, Y.; Glotzer, S. C.; Kotov, N. A. *Science* **2006**, *314*, 274–278.
(20) Qu, L. H.; Peng, X. G. *J. Am. Chem. Soc.* **2002**, *124*, 2049–2055.
(21) Zeng, J.; Lu, W.; Wang, X.; Wang, B.; Wang, G.; Hou, J. G. *J. Colloid Interface Sci.* **2006**, *298*, 685–688.
(22) Arnold, D. R.; Wong, P. C. *J. Am. Chem. Soc.* **1977**, *99*, 3361–3366.
(23) Pokropivny, V. V. *Powder Metall. Met. Ceram.* **2001**, *40*, 582–594.
(24) Tenne, R. *Angew. Chem., Int. Ed.* **2003**, *42*, 5124–5132.
(25) Shannon, R. D. *Acta Crystallogr., Sect. A: Found. Crystallogr.* **1976**, *32*, 751–767.
(26) Mayers, B.; Jiang, X.; Sunderland, D.; Cattle, B.; Xia, Y. N. *J. Am. Chem. Soc.* **2003**, *125*, 13364–13365.
(27) Yang, P. D. *Nature* **2003**, *425*, 243–244.

NL0733334